Sidelobe Control in Collaborative Beamforming via Node Selection

Mohammed F. A. Ahmed, *Student Member, IEEE*, and Sergiy A. Vorobyov, *Senior Member, IEEE*

***Abstract*—Collaborative beamforming (CB) is a power efficient method for data communications in wireless sensor networks (WSNs) which aims at increasing the transmission range in the network by radiating the power from a cluster of sensor nodes in the directions of the intended base stations or access points (BSs/APs). The CB average beampattern shows a deterministic behavior and the mainlobe of the CB sample beampattern is independent of the particular node locations. However, the CB for a cluster of a finite number of collaborative nodes results in a sample beampattern with sidelobes that severely depend on the particular node locations. High level sidelobes can cause unacceptable interference when they occur at directions of unintended BSs/APs. Therefore, sidelobe control in CB has a potential to decrease the interference at unintended BSs/APs and increase the network transmission rate by enabling simultaneous multilink CB. Traditional sidelobe control techniques are proposed for centralized antenna arrays and are not suitable for WSNs. In this paper, we show that scalable and low-complexity sidelobe control techniques suitable for CB in WSNs can be developed based on a node selection technique which makes use of the randomness of the node locations. A node selection algorithm with low-rate feedback is developed to search over different node combinations. The performance of the proposed algorithm is analyzed in terms of the average number of search trials required for selecting the collaborative nodes, the resulting interference, and the corresponding transmission rate improvements. Our simulation results show that the interference can be significantly reduced and the transmission rate can be significantly increased when node selection is implemented with CB. The simulation results also show close agreement with our theoretical results.**

***Index Terms*—Collaborative beamforming, node selection, sidelobe control, wireless sensor networks.**

I. Introduction

WIRELESS sensor networks (WSNs) are increasingly employed in different applications such as habitat and climate monitoring, detection of human/vehicular intrusion, and others [1]. Such applications require low-power sensor nodes with simple hardware to be deployed over a remote area to collect data from the surrounding environment and send it to far base stations or access points (BSs/APs). As a result, the challenges for data communications in WSNs are quite different from that of considered in traditional wireless ad-hoc networks [2]. Practical communication schemes for WSNs should overcome the problem of limited transmission range of individual sensor nodes, while being distributed and scalable. Moreover, for designing such communication schemes, power consumption and implementation complexity issues have to be taken into account as the most significant design constraints for WSNs.

To address the aforementioned issues, the inherent high density deployment of sensor nodes has been used to introduce collaborative beamforming (CB) for the uplink communication to a BS/AP [3] (see also [4]). CB extends the transmission range of sensor nodes by using a cluster of sensor nodes jointly for transmission. Particularly, sensor nodes from one cluster act collaboratively as distributed antenna array and adjust the initial phases of their carriers so that the individual signals from different sensor nodes add constructively and form a beam toward the directions of the intended BSs/APs. In this way, CB is able to increase the transmission range of sensor nodes and, in some applications, it can be also viewed as an alternative scheme to the multihop relay communications.

In order to implement CB, distributed schemes for estimating the initial phases of the local node oscillators in WSNs have been introduced in [5]–[7]. A synchronization algorithm developed in [5] uses a simple 1-bit feedback iterations, while other methods developed in [6] and [7] are based on the time-slotted round-trip carrier synchronization approach. To minimize the time required for multiple sources for sharing the data among all sensor nodes in a cluster, a medium access control-physical (MAC-PHY) cross-layer CB scheme which is based on the medium random access has been proposed in [8].

One more concern of the CB design is the uncontrolled sidelobes of the sample beampattern due to the random sensor node locations. The effect of the spatial sensor node distribution on the characteristics of the CB beampattern has been studied in [3] (see also [9] and [10]) for the case of sensor nodes with uniform spatial distribution and in [4], [11] for the case of sensor nodes with Gaussian spatial distribution. Although it has been shown for both aforementioned node distributions that the CB sample beampattern has a deterministic mainlobe which is independent of the random sensor node locations, the sidelobes of the CB sample beampattern are random and can be described only in statistical terms [3], [4], [12]. In addition, the aforementioned multiple access scheme of [8] results in higher sidelobes even for the average CB beampattern. All these reasons can lead to high interference levels at the directions of unintended BSs/APs. Therefore, the sidelobe control problem arises

Manuscript received December 07, 2009; accepted September 05, 2010. Date of publication September 20, 2010; date of current version November 17, 2010. The associate editor coordinating the review of this paper and approving it for publication was Dr. Martin Schubert. This work was supported in part by the Natural Sciences and Engineering Research Council (NSERC) of Canada and in part by the Alberta Innovates—Technology Futures, Alberta, Canada. The material in this paper was presented at the IEEE Workshop on Signal Processing Advances in Wireless Communications (SPAWC), Perugia, Italy, 2009.

The authors are with the Department of Electrical and Computer Engineering, University of Alberta, Edmonton, AB, T6G 2V4 Canada (e-mail: mfahmed@ece.ualberta.ca; vorobyov@ece.ualberta.ca).

Digital Object Identifier 10.1109/TSP.2010.2077631

for CB in the context of WSNs. Indeed, lower interference at unintended BSs/APs archived by the sidelobe control has the potential to increase the WSN transmission rate by enabling multilink CB. The problem of high sidelobe levels of the average CB beampattern has been mentioned in [13]. It is suggested in [13] to use only sensor nodes placed in multiple concentric rings instead of using all nodes in the coverage area to achieve higher directivity. However, a narrower ring with larger radius results in the average beampattern with narrower mainlobe and leads to larger sidelobe peak levels in some directions. Moreover, only the average beampattern behavior is considered in [13], while it is the sample beampattern behavior that is of practical concern for the sidelobe control in WSNs.

Due to the inherent distributed nature of WSNs, the sidelobe control has to be achieved with minimum data overhead and knowledge of the channel information. Unfortunately, traditional sidelobe control techniques developed in classical array processing [14]–[17] cannot be applied in the context of WSNs due to their unacceptably high complexity and the requirement of centralized processing. Indeed, to apply the centralized beamforming weight design in the WSNs, a node or BS/AP has to collect the location and channel information from all sensor nodes and, thus, significantly increase the corresponding overhead in the network. Note that for the same reasons, the recently developed network beamforming techniques [2], [18] are restricted to the applications in the relay networks only.

In this paper[1], we formulate and study the sidelobe control problem in the CB sample beampattern using node selection. It enables us to introduce the interference reduction capabilities for WSNs, which in turns, enables multilink CB versus the single-link CB of [3] and [4]. The enabling concept for achieving sidelobe control by node selection is the randomness of the node locations in WSNs. Indeed, different combinations of sensor nodes result in beampatterns with different sidelobes. Typical WSNs consist of hundreds or thousands of sensor nodes that guarantees that a large range of sidelobe levels can be achieved by simply selecting different combinations of sensor nodes. Selecting different combinations of nodes is equivalent to assigning different beamforming weights, which are determined by node locations and corresponding channel gains. Therefore, the beamforming design boils down to selection of an acceptable combination of such weights. Thus, we develop a random node selection algorithm with low-rate feedback. As compared to the optimal beamforming weights design, our algorithm does not depend on channel gain measurements/estimates and does not suffer from the finite precision problem related to the need of communicating the channel gain to a central point. Thus, it suits well the WSN applications since it avoids complex computations and additional communications accompanied by central beamforming weight design. Note that a central point is still required for performing the scheduling functions to arrange the order of node selection or order of communication with the BSs/APs. Such scheduling functions are, however, much simpler than the central beamforming weights design. Note also that a similar technique based on random selection is used in other signal processing problems such as, for example, multiple choice sequences for OFDM [20]. The performance of the proposed algorithm is analyzed in terms of: (i) the average number of trials required to select collaborative nodes; (ii) the distribution of the resulting interference; and (iii) the corresponding average signal-to-interference-plus-noise ratio (SINR) and transmission rate.

[1]Some preliminary results have been also reported in [19].

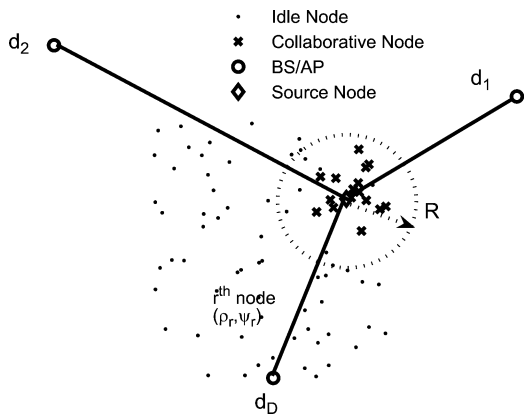

Fig. 1. WSN model with multiple BSs/APs.

The rest of the paper is organized as follows. System and signal models are introduced in Section II. A new sidelobe control technique for CB in WSNs based on node selection is developed in Section III. The performance of the proposed technique is studied in Section IV. Section V reports our simulation results and is followed by conclusions in Section VI. This paper is reproducible research [21] and the software needed to generate the numerical results of this paper can be obtained from www.ece.ualberta.ca/~vorobyov/SensSel.rar.

II. System and Signal Model

A. System Model

We consider a WSN with sensor nodes randomly placed over a plane as shown in Fig. 1. Multiple BSs/APs, denoted as $\mathcal{D} = \{d_0, d_1, \ldots, d_D\}$, are located outside and far apart from the coverage area of each individual node at directions $\varphi_0, \varphi_1, \ldots, \varphi_D$, respectively. Due to limited power of individual sensor nodes, direct transmission to the BSs/APs is impossible and sensor nodes have to employ CB for uplink transmission. Uplink transmission is a burst traffic for which the nodes are idle most of the time and have sudden transmissions. Thus, a time-slotted transmission scheme, where nodes are allowed to transmit at the beginning of each time slot, can be, for example, adopted. The downlink transmissions from different BSs/APs are only control data broadcasted over separate error-free control channels. In practice, the BSs/APs typically can be connected to each other with almost no delay communication links and can simply use one control channel. The BSs/APs can use high power transmission and, therefore, the downlink is less challenging and can be organized as direct transmission. The distance between nodes in one cluster of WSN is small so that the power consumed for communication among sensor nodes can be neglected. Each sensor node is equipped with a single antenna used for both transmission and reception. To identify different nodes in a cluster, each node

has a unique identification (ID) sequence that is included in each transmission.

At each time slot, a set $\mathcal{S} = \{s_0, s_1, \ldots, s_S\}$ of source nodes is active. However, only $K+1$ source–destination pairs are allowed to communicate[2]. Here $K+1 = \min\{\mathrm{card}(\mathcal{S}), \mathrm{card}(\mathcal{D})\}$ where $\mathrm{card}(\cdot)$ denotes the cardinality of a set, and the kth source–destination pair is denoted as $s_k - d_k$. For source node s_k, the coverage area is, ideally, a circle with a radius which depends on the power allocated for the node-to-node communication.

Let $\mathcal{M}^k$ be a set of nodes in the coverage area of the node s_k. Then the rth collaborative node, denoted as c_r, $r \in \mathcal{M}^k$, has polar coordinates (ρ_r, ψ_r) relative, for example, to the source node s_k. The Euclidean distance between the collaborative node c_r and a point (A, ϕ) in the same plane is given as

$$d_r(\phi) \triangleq \sqrt{A^2 + \rho_r^2 - 2\rho_r A\cos(\phi - \psi_k)} \approx A - \rho_r \cos(\phi - \psi_r) \quad (1)$$

where $A \gg r_k$ in the far-field region.

The array factor for the set of sensor nodes $\mathcal{M}^k$ in a plane can be defined as

$$AF^k(\phi) \triangleq \sum_{r\in\mathcal{M}^k} \sqrt{P_r} e^{j\theta_r^k} e^{-j\theta_r(\phi)} \quad (2)$$

where P_r is the transmit power of the rth node, θ_r^k is the initial phase of the rth sensor carrier frequency, $\theta_r(\phi) = (2\pi/\lambda)d_r(\phi)$ is the phase delay due to propagation at the point (A, ϕ), and λ is the wavelength of the carrier. Then the far-field beampattern corresponding to the set of sensor nodes $\mathcal{M}^k$ can be found as

$$BP^k(\phi) \triangleq \left|AF^k(\phi)\right|^2 = \left|\sum_{r\in\mathcal{M}^k} \sqrt{P_r} e^{j\theta_r^k} e^{-j\theta_r(\phi)}\right|^2 \quad (3)$$

where $|\cdot|^2$ denotes the magnitude of a complex number. The mainlobe of the beampattern is formed toward the direction of d_k while collaborative node $c_r, r \in \mathcal{M}^k$ is synchronized with the initial phase $\theta_r^k = -(2\pi/\lambda)\rho_r\cos(\varphi_k - \psi_r)$ using the knowledge of the node location (see the closed-loop scenario in [3]). Alternatively synchronization can be performed without any knowledge of the node locations [5]–[7]. Note that the synchronization step has to be done at the network deployment stage to enable CB irrespective to whether it is the single-link CB of [3] and [4] or the multilink CB of this paper. Synchronization with multiple BSs/APs is a straightforward process with overhead increasing only linearly with the number of the BSs/APs.

The channel characteristics near ground in outdoor WSN applications of interest, i.e., the scenarios in which CB is needed, suggest that the channel attenuation varies very slowly with time [22], [23]. Therefore, the channel variations over time can be neglected and the channel can be considered to be time-invariant. Moreover, the large-scale fading is the dominant factor for the channels between collaborative nodes in $\mathcal{M}^k$ and BSs/APs. Then the channel coefficient for rth collaborative node which serves kth source–destination pair can be modeled as $h_{rk} = a_{rk}b_{rk}$. Here a_{rk} is assumed to be a lognormal distributed random variable which represents the fluctuation/shadowing effect in the channel coefficient, i.e., $a_{rk} \sim \exp\{\mathcal{N}(0, \sigma^2)\}$, where σ^2 is the variance of the corresponding zero-mean Gaussian distribution (see [24, p. 9]). The other factor b_{rk} is the attenuation/path loss effect in the channel due to propagation distance. Thus, it depends on the distance between c_r and d_k and the path loss exponent. Assuming that all nodes in $\mathcal{M}^k$ are close to each other, the pass loss from the nodes in $\mathcal{M}^k$ to the BS/AP d_k are equal to each other, i.e., $b_{rk} = b_k$, $r \in \mathcal{M}^k$ [25]. Moreover, since all BSs/APs are located far apart from the cluster of collaborative nodes, the network can be viewed as homogeneous and the attenuation effects of different paths can be assumed approximately equal to each other, i.e., $b_k = b$ [26]. Note that even if the attenuation effects for different BSs/APs are different, they can be compensated by adjusting the gains of the corresponding receivers or the power/number of the corresponding collaborative nodes participating in CB. Therefore, the channel model simplifies to $h_{rk} = a_{rk}$.

B. CB and Corresponding Signal Model

Consider a two-step transmission which consists of the information sharing and the actual CB steps. Information sharing aims at broadcasting the data from one source node to all other nodes in its coverage area. Specifically, in this step, the source node s_k broadcasts the data symbol z_k to all nodes in its coverage area $\mathcal{M}^k$, where the data symbol $z_k \in \mathbb{C}$ belongs to a codebook of zero mean, unit power, and independent symbols, i.e., $E\{z_k\} = 0$, $|z_k^2| = 1$, and $E\{z_k z_n\} = 0$ for $n \neq k$, where $E\{\cdot\}$ stands for the statistical expectation.

In the case of multiple source nodes, data sharing can be achieved over orthogonal channels in frequency, time, or code to avoid collisions. Note that the use of time orthogonal channels requires scheduling which can be achieved by an appropriate MAC protocol or using the BSs/APs as a central scheduler. Alternatively, the existing collision resolution schemes can be used [27], [28].

We assume that the power used for broadcasting the data by the source node is high enough so that each collaborative node c_r can successfully decode the received symbol from the source node s_k. During the CB step, each collaborative node c_r, $r \in \mathcal{M}^k$ targeting d_k transmits the signal

$$t_r = z_k \sqrt{P_r}\, e^{j\theta_r^k}, \quad r \in \mathcal{M}^k. \quad (4)$$

Then the received signal at angle ϕ from all collaborative sets $\mathcal{M}^k$, $\forall k \in \{0, 1, \ldots, K\}$ can be written as

$$g(\phi) = \sum_k z_k \sum_{r\in\mathcal{M}^k} \sqrt{P_r}\, a_{rk}\, e^{j\theta_r^k}\, e^{-j\theta_r(\phi)} + w \quad (5)$$

where $w \sim \mathcal{CN}(0, \sigma_w^2)$ is the additive white Gaussian noise (AWGN) at the direction ϕ. The received noise power σ_w^2 at BSs/APs can be measured in the absence of data transmission and, therefore, is assumed to be known at each BS/AP.

[2]This can be organized at the higher media access layer through scheduling or random access protocol. For example, BSs/APs can simply perform the scheduling function.

The received signal at the BS/AP d_{k^*} can be written as

$$\begin{aligned} g_{k^*} &\triangleq g(\varphi_{k^*}) \\ &= z_{k^*} \sum_{r\in\mathcal{M}^{k^*}} \sqrt{P_r} a_{rk^*} \\ &\quad + \sum_{k\neq k^*} z_k \sum_{r\in\mathcal{M}^k} \sqrt{P_r} a_{rk^*} e^{-j(\theta_r^{k^*}-\theta_r^k)} + w \\ &= z_{k^*} \sum_{r\in\mathcal{M}^{k^*}} \sqrt{P_r} a_{rk^*} \\ &\quad + \sum_{k\neq k^*} z_k \sum_{r\in\mathcal{M}^k} \sqrt{P_r} a_{rk^*} \left(x_r^{(k^*,k)} - j y_r^{(k^*,k)} \right) + w \end{aligned} \tag{6}$$

where $x_r^{(k^*,k)} = \mathcal{R}\left\{e^{-j(\theta_r^{k^*}-\theta_r^k)}\right\}$ and $y_r^{(k^*,k)} = \mathcal{I}\left\{e^{-j(\theta_r^{k^*}-\theta_r^k)}\right\}$ while $\mathcal{R}\{\cdot\}$ and $\mathcal{I}\{\cdot\}$ represent the real and the imaginary parts of a complex number, respectively. As shown in [4], the array factor has a random behavior on the sidelobe region[3] and, therefore, $x_r^{(k^*,k)}$ and $y_r^{(k^*,k)}$ are independent random variables. It can be further shown that $u \in \left\{x_r^{(k^*,k)}, y_r^{(k^*,k)}\right\}$ has mean $m_{x_r^{(k^*,k)}} = m_{y_r^{(k^*,k)}} = m_u = E\{u\} = 0$ and variance $\sigma^2_{x_r^{(k^*,k)}} = \sigma^2_{y_r^{(k^*,k)}} = \sigma_u^2 = E\{u^2\} = 0.5$ (see Appendix A). Moreover, the first term in (6) is the signal received at the BS/AP d_{k^*} from the desired set of collaborative nodes $\mathcal{M}^{k^*}$ and the second term represents the interference caused by other sets of nodes $\mathcal{M}^k$, $\forall k \neq k^*$ with $\mathcal{M}^k \cap \mathcal{M}^n = \varnothing$, $k \neq n$.

III. Sidelobe Control via Node Selection

As mentioned before, the randomness of the node locations provides additional degrees of freedom for controlling the beampattern sidelobes. Thus, to achieve desired sidelobes, it is required to select a subset of collaborative nodes from the candidate nodes in the coverage area of each source node. Node selection is performed at the network deployment stage and is repeated only when the network configuration changes. Note that the selection process can not be done during data transmission and, if needed, any BS/AP can stop the transmission for all collaborative nodes at any time to perform node selection and then continue the transmission after.

Let $\mathcal{N}^k$ be a set of collaborative nodes to be selected from $\mathcal{M}^k$, i.e., $\mathcal{N}^k \subset \mathcal{M}^k$, to beamform data symbols to d_k. We aim at assigning a set of collaborative nodes $\mathcal{N}^k \subset \mathcal{M}^k$ to each source–destination pair $s_k - d_k$. Note that according to [3] and [4], the mainlobe of the beampattern is stable for different subsets of $\mathcal{M}^k$ as long as the coverage area does not change and each cluster of the WSN consists of a sufficiently large number of sensor nodes. To achieve a beampattern with low level sidelobes toward the unintended BSs/APs, we develop a low-complexity node selection algorithm, which guarantees that the sidelobe levels at the directions of the unintended BSs/APs are below a certain prescribed value(s). Such algorithm should utilize only the knowledge of the receive interference-to-noise ratio (INR), denoted as η, at the unintended destinations and requires only low-rate (essentiality, one-bit) feedback from the unintended BSs/APs at each trial.

To select such a collaborative set, the nodes can be tested one by one or a group of nodes by a group of nodes. The latter is preferable since it can significantly reduce the data overhead in the system. Indeed, while testing one node or a group of nodes, we need to check if the corresponding CB sample beampattern sidelobe level reduces in the unintended direction(s) and then send one 'approve/reject' bit per one node in the first case, or per a group of nodes in the second case. Therefore, if every group of nodes consists of a larger number of sensor nodes, less 'approve/reject' bits have to be sent in total. Note that the node selection is performed for one source–destination pair at a time and a schedule that arranges the source nodes order in the node selection process is maintained by the BSs/APs or a MAC protocol. Moreover, only nodes that are not assigned to any other source–destination pairs are available as candidate nodes for selection.

Consider the source node s_{k^*}, let the number of nodes in its coverage area be M, the number of collaborative nodes needed to be selected be $N \leq M$, and the size of one group of nodes to be tested in each trial be $L \leq N$. Using the selection principle highlighted above, the selection process can be organized in the following two steps.

Step 1: Selection. Source node s_{k^*} initiates the node selection by broadcasting the *select message* to the nodes in its coverage area, namely the set $\mathcal{M}^{k^*}$, and randomly selects a subset $\mathcal{L}^{k^*}$ of L candidate nodes from $\mathcal{M}^{k^*}$.

Nodes can be assigned to the set $\mathcal{L}^{k^*}$ by using any of the following two methods. The first one is a centralized method in which the source node s_{k^*} maintains a table of IDs of all candidate nodes in its coverage area and broadcasts the IDs of the nodes randomly assigned to the set $\mathcal{L}^{k^*}$. The disadvantage of this method is that each source node has to keep records of all other nodes in its coverage area. Moreover, this method requires extensive data exchange between the source and candidate nodes and, therefore, is suitable only for small WSNs.

Alternatively, in the second method, node assignment task is distributed among the source and collaborative nodes. In particular, if collaborative nodes receive the *select message*, each node starts a random delay using an internal timer. After the random delay, the candidate node responds by the *offer message* which contains the ID of this node. Then the source node responds by the *approval message* which requires only 1 bit of feedback. If a collision occurs and two collaborative nodes transmit the *offer message* at the same time, the source node responds by the *approval message* with a different bit value and the timers in both nodes start over new random delays. The process repeats and the source node s_{k^*} keeps sending the *select message* until L candidate nodes are assigned and the set $\mathcal{L}^{k^*}$ is constructed. Assignment of $\mathcal{L}^{k^*}$ can be performed in one time-slot by setting the limits of random timer appropriately, so that the candidate set $\mathcal{L}^{k^*}$ is ready for transmission at the beginning of the next time slot.

Step 2: Test. Once the candidate subset $\mathcal{L}^{k^*}$ is assigned, it transmits a *test message* containing the intended BS/AP ID at the beginning of the next time-slot to the intended destination d_{k^*} using CB. While the intended destination d_{k^*} receives a

[3]It is worth noting that in typical WSNs, there is no need to put BSs/APs close to each other and BSs/APs are well separated. Therefore, when forming a beampattern with a mainlobe towards certain BS/AP, other unintended BSs/APs will be in the sidelobe region of that beampattern.

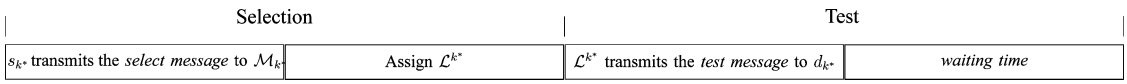

Fig. 2. Timing diagram for node selection process.

TABLE I
NODE SELECTION ALGORITHM FOR CB SIDELOBE CONTROL

Node selection algorithm
Initial values:
N and L are predetermined at the Source Node s_{k^*}.
η_{thr} is predetermined at the unintended Destinations d_k, $k = \{0, 1, \ldots, D\}$.
1: At s_{k^*}: (Counter $l \leftarrow 1$).
2: **If** (Counter $l < \frac{N}{L}$),
3: **Then:** { s_{k^*} broadcasts the *select message*.
4: A candidate set $\mathcal{L}_l^{k^*}$ is constructed.
5: Using CB, the nodes in $\mathcal{L}_l^{k^*}$ transmit the *test message*.}
6: **Otherwise:** {Go to 12.}
7: At any $d_k, \forall k \neq k^*$: **If** (The receive INR $\eta > \eta_{\text{thr}}$),
8: **Then** { d_k sends the *reject message* to $\mathcal{L}_l^{k^*}$.}
9: **Else** { No *reject message* is received.
10: $\mathcal{L}_l^{k^*}$ is approved and the corresponding nodes store the IDs of s_{k^*} and d_{k^*}.
11: At s_{k^*}: (Counter $l \leftarrow$ Counter $l + 1$). **Go to** 2.}
12: s_{k^*} broadcasts the *end message*.

predetermined signal power level, the interference power levels at the unintended destination(s) d_k, $\forall k \neq k^*$ are random because of the random sidelobes of the CB beampattern. At this step, all unintended BSs/APs with different IDs measure the received INR η. If η is higher than a predetermined threshold value η_{thr}, the *reject message* is sent back to the candidate set $\mathcal{L}^{k^*}$. If multiple BSs/APs send *reject messages*, only the first *reject message* is sufficient to reject the candidate set. Other possibility is that BSs/APs coordinate transmissions and only one *reject message* is transmitted for multiple BSs/APs. In this case, the nodes in the candidate set $\mathcal{L}^{k^*}$ are all returned to the set of nodes $\mathcal{M}^{k^*}$ and can be used in future trials. If no *reject message* is received from any of the unintended BSs/APs after a predetermined *waiting time*, then the candidate set $\mathcal{L}^{k^*}$ is approved and each node from $\mathcal{L}^{k^*}$ stores the IDs of the source node s_{k^*} and the destination d_{k^*}. Then the collaborative nodes assigned to serve the source–destination pair $s_{k^*} - d_{k^*}$ do not participate in future trials. In this way, we can avoid any overlap between sets of nodes serving different BSs/APs. Note that the *waiting time* has to be set long enough so that the BSs/APs can measure the INR over longer time to assure that the INR variations are in an acceptable range.

In order to select N collaborative nodes, the Selection and Test steps are repeated until N/L candidate sets $\mathcal{L}_l^{k^*}$, $l = 1, 2, \ldots, N/L$, are approved.[4] Then the so obtained set of approved collaborative nodes is $\mathcal{N}^{k^*} = \bigcup_l \mathcal{L}_l^{k^*}$. Once $\mathcal{N}^{k^*}$ is constructed, the source node s_{k^*} broadcasts the *end message*. The timing diagram of the node selection process is shown in Fig. 2 and the pseudocode of the node selection algorithm is also given in Table I.

Although the proposed node selection strategy does not guarantee the optimal result of centralized beamforming strategies (which require global knowledge of the channel information and, therefore, a very significant data overhead in the network), it has practically important advantages for WSNs since it can be run in sensor nodes with simple hardware, it is scalable and uses minimum control feedback from the unintended BSs/APs. Finally, note that once the collaborative nodes are assigned for each source node, the links between different source—destination pairs have minimum interference to each other and are independent. Then the actual data communication is a directional (unicast) transmission to a specific BSs/APs which can be straightforwardly implemented based on scheduling or any appropriate random access protocol.

IV. PERFORMANCE ANALYSIS

In this section, we analyze the proposed node selection algorithm in terms of: (i) the average number of trials required for selecting a set of collaborative nodes; (ii) the complementary cumulative distribution function (CCDF) of the received INR η; and (iii) the achievable average SINR and corresponding transmission rate. The first characteristic allows to estimate the average run time of the algorithm, while the second characteristic

[4]It is assumed for simplicity that N/L is an integer number. If N/L is not integer, it is still easy to adjust the size of the candidate set $\mathcal{L}^{k^*}$ in the last trial of the algorithm only.

is needed to estimate the achievable interference levels versus the corresponding interference threshold values. The achievable average SINR and transmission rate aim at emphasizing the improvements that the multilink CB with node selection provides as compared to the multilink CB without node selection and single-link CB of [3] and [4]. For simplicity, but without loss of generality, we assume in our further analysis that each node in the network utilizes the same amount of power for each CB transmission, i.e., $P_r = P,\ \forall r$ in (6).[5]

A. Average Number of Trials

It is worth reminding that the node selection for the set $\mathcal{N}^{k^*}$ which serves the link $s_{k^*} - d_{k^*}$ is performed for one source–destination pair at a time. We assume that the total transmit power budget for each tested candidate set of nodes is kept the same in each trial of CB transmission for any number of collaborative nodes. In particular, the power per one sensor node in $\mathcal{L}_l^{k^*}$ has to be set as $P = \sigma_w^2\gamma/L$ in the selection process, where γ is the power budget for single CB transmission normalized to σ_w^2. Then the signal-to-noise ratio (SNR) at the intended BS/AP is $10\log_{10}(L\gamma)$ dB where L is the corresponding array gain. The power consumed for running the node selection algorithm is proportional to the average number of trials in the algorithm. Therefore, it is preferable to construct a set of collaborative nodes with less number of trials.

In order to derive the average number of trials for the node selection algorithm, we, first, need to find the probability that a candidate set of nodes $\mathcal{L}_l^{k^*}$ is approved as part of the set of collaborative nodes $\mathcal{N}^{k^*}$. This probability is the same as the probability that the set $\mathcal{L}_l^{k^*}$ generates an acceptable interference at the unintended BSs/APs. Since we assumed that only one set of collaborative nodes $\mathcal{N}^{k^*}$ is constructed at a time, there is no interference present from other candidate sets. Using (6), the interference power received at the unintended BS/AP d_k from the tested candidate set of nodes $\mathcal{L}_l^{k^*}$ which targets the intended BS/AP d_{k^*} can be written as

$$I\left(\varphi_k \left| \mathcal{L}_l^{k^*}\right.\right) = \sqrt{\frac{\sigma_w^2\gamma}{L}} z_{k^*} \sum_{r\in\mathcal{L}_l^{k^*}} a_{rk}\left(x_r^{(k^*,k)} - jy_r^{(k^*,k)}\right) = z_{k^*}\left(X_l^{(k^*,k)} - jY_l^{(k^*,k)}\right) \tag{7}$$

where $X_l^{(k^*,k)} \triangleq \sqrt{\sigma_w^2\gamma/L}\sum_{r\in\mathcal{L}_l^{k^*}} a_{rk}x_r^{(k^*,k)}$ and $Y_l^{(k^*,k)} \triangleq \sqrt{\sigma_w^2\gamma/L}\sum_{r\in\mathcal{L}_l^{k^*}} a_{rk}y_r^{(k^*,k)}$ can be approximated by zero-mean Gaussian random variables with $\sigma_X^2 = \sigma_Y^2 = \gamma\sigma_w^2\sigma_u^2\left(\sigma_a^2 + m_a^2\right)$ (see [3]), and m_a and σ_a^2 are the mean and variance of the lognormal distributed a_{rk} (see [24, p. 9] for the corresponding expressions).

Using (7) and the fact that $|z_{k^*}|^2 = 1$, the received interference power at the unintended BS/AP d_k from the candidate set of nodes $\mathcal{L}_l^{k^*}$ can be expressed as

$$\left|I\left(\varphi_k \left| \mathcal{L}_l^{k^*}\right.\right)\right|^2 = \left(X_l^{(k^*,k)}\right)^2 + \left(Y_l^{(k^*,k)}\right)^2. \tag{8}$$

[5]The general case straightforwardly follows from our analysis by substituting corresponding P_r's $\forall r$.

Then the probability that the candidate set of nodes $\mathcal{L}_l^{k^*}$ is approved to join the set of collaborative nodes $\mathcal{N}^{k^*}$, i.e., the probability that the INR η from $\mathcal{L}_l^{k^*}$ at the unintended BS/AP d_k is lower than the threshold value $\eta_{\rm thr}$, can be found as

$$\begin{aligned} p' &\triangleq \mathbf{Pr}\left\{\eta < \eta_{\rm thr}\right\} \\ &= \mathbf{Pr}\left\{\frac{\left|I(\varphi_k \left| \mathcal{L}_l^{k^*}\right.)\right|^2}{\sigma_w^2} < \eta_{\rm thr}\right\} \\ &= \mathbf{Pr}\left\{\frac{\left(X_l^{(k^*,k)}\right)^2 + \left(Y_l^{(k^*,k)}\right)^2}{\sigma_w^2} < \eta_{\rm thr}\right\} \\ &= 1 - \exp\left(-\frac{\eta_{\rm thr}\sigma_w^2}{2\sigma_X^2}\right) \end{aligned} \tag{9}$$

where the INR $\eta = \left(\left(X_l^{(k^*,k)}\right)^2 + \left(Y_l^{(k^*,k)}\right)^2\right)\Big/\sigma_w^2$ is exponentially distributed random variable with the probability density function (pdf)

$$f\left(\eta \;\middle|\; \frac{\sigma_w^2}{2\sigma_X^2}\right) = \begin{cases} \frac{\sigma_w^2}{2\sigma_X^2}\exp\left\{-\frac{\sigma_w^2\eta}{2\sigma_X^2}\right\}, & \eta \geq 0 \\ 0, & \eta < 0. \end{cases} \tag{10}$$

It is worth noting that any value of $\eta_{\rm thr}$ in the distribution range of the INR η will result in non-zero value of p'. Indeed, the interference power $\left|I\left(\varphi_k \left| \mathcal{L}_l^{k^*}\right.\right)\right|^2$ depends on the set $\mathcal{L}_l^{k^*}$. Although the number of possible combinations for constructing $\mathcal{L}_l^{k^*}$ is finite, it equals to $\binom{M}{L} = M!/L!(M-L)!$, which is very large number for typical WSNs consisting of hundreds or thousands of sensor nodes.[6] Different values of the interference power $\left|I\left(\varphi_k \left| \mathcal{L}_l^{k^*}\right.\right)\right|^2$, which correspond to different combinations of $\mathcal{L}_l^{k^*}$, cover the same range of the beampattern levels that can be achieved using L collaborative nodes. Once we set $\eta_{\rm thr}$ to a value from that achievable range of beampattern levels, the number of trials for selecting $\mathcal{N}^{k^*}$ should be finite.

It is also important to note that $X_l^{(k^*,k)}$ and $Y_l^{(k^*,k)}$ are defined through the independent random variables $x_r^{(k^*,k)}$ and $y_r^{(k^*,k)}$, respectively, and the channel gains a_{rk} which are also independent random variables for different directions $\varphi_k,\ \forall k \neq k^*$. Therefore, $X_l^{(k^*,k)}$ and $Y_l^{(k^*,k)}$ are independent random variables $\forall k \neq k^*$ and the interference levels caused by $\mathcal{L}_l^{k^*}$ at different directions $\varphi_k,\ \forall k \neq k^*$, $\left|I\left(\varphi_k \left| \mathcal{L}_l^{k^*}\right.\right)\right|^2$, are also independent random variables. If D unintended BSs/APs are present in the neighborhood of the set of candidate collaborative nodes $\mathcal{L}_l^{k^*}$, the probability that the INR from $\mathcal{L}_l^{k^*}$ at any one of these unintended BSs/APs is lower than the threshold value $\eta_{\rm thr}$ is given by (9). Therefore, the probability that $\mathcal{L}_l^{k^*}$ is approved by all BSs/APs is the product of the probabilities that $\mathcal{L}_l^{k^*}$ is approved by each of the unintended BSs/APs, that is

$$p = \left(1 - \exp\left(-\frac{\eta_{\rm thr}\sigma_w^2}{2\sigma_X^2}\right)\right)^D. \tag{11}$$

It can be seen from (11) that p decreases if the threshold $\eta_{\rm thr}$ decreases or the number D of unintended BSs/APs increases.

[6]For example, if 256 candidate nodes have to be selected from 512 nodes, the number of combinations is 4.7255×10^{152} each corresponding to different value of the beampattern levels.

Using (11), a closed-form expression for the average number of trials can be derived. Since the candidate nodes are selected randomly at each trial, the algorithm itself can be viewed as a Bernoulli process. Since $T_0 = N/L$ of these Bernoulli trials must be successful among the first T trials in order to construct $\mathcal{N}^{k^*}$, the probability distribution of the number of trials T is, in fact, negative binomial distribution, that is

$$\mathbf{Pr}\{T=t\} = \binom{t-1}{T_0-1} p^{T_0}(1-p)^{t-T_0}. \tag{12}$$

Using (12) and the expression for the mean of the negative binomial distribution [29, p. 82], the average number of trials for the proposed node selection algorithm can be obtained as

$$E\{T\} = \frac{T_0}{p} = \frac{N}{L\cdot p}. \tag{13}$$

It can be seen from (13) that the average number of trials is proportional to the size of the set of collaborative nodes $\mathcal{N}^{k^*}$, but it is inverse proportional to the size of the candidate set of nodes $\mathcal{L}_l^{k^*}$ and to the probability that the set $\mathcal{L}_l^{k^*}$ is approved to join the set $\mathcal{N}^{k^*}$. Therefore, less number of trials is required in average for the proposed node selection algorithm if L is chosen to be large for a certain value of N. Moreover, if the probability p is large, then less number of trials is required.

B. CCDF of Interference

Once the collaborative nodes are assigned for each source—destination pair, the links between different source—destination pairs have minimum interference to each other and can be used independently for the multilink CB. In this subsection, we study the CCDF of the interference occurring during simultaneous multilink CB communications of $K+1$ different source—destination pairs. At the intended destination d_{k^*}, other K collaborative sets that target different d_k, $\forall k \neq k^*$ destinations are interfering. These sets are $\mathcal{N}^k$, $\forall k \neq k^*$ and their union is denoted hereafter as $\bigcup \mathcal{N}^{k\neq k^*}$. Using (7), the total interference collected at the destination d_{k^*} from all K interfering collaborative sets can be expressed as

$$I\left(\varphi_{k^*}\left|\bigcup \mathcal{N}^{k\neq k^*}\right.\right) = \sqrt{\frac{\sigma_w^2\gamma}{N}} \sum_{k\neq k^*} z_k \sum_{r\in\mathcal{N}^k} a_{k^*r}\left(x_r^{(k^*,k)} - j y_r^{(k^*,k)}\right) \tag{14}$$

where the power per one collaborative sensor node is $P = \sigma_w^2\gamma/N$ in this case, and the SNR at the intended BS/AP is $10\log_{10}(N\gamma)$ dB. Using the fact that $\mathcal{N}^k = \bigcup \mathcal{L}_l^k$ and multiplying and dividing the right-hand side (RHS) of (14) by $\sqrt{L}$, the total interference at d_{k^*} can be expressed as

$$\begin{aligned} I\left(\varphi_{k^*}\left|\bigcup \mathcal{N}^{k\neq k^*}\right.\right) &= \sqrt{\frac{L}{N}} \sum_{k\neq k^*} z_k \sum_{l=1}^{N/L} \sum_{r\in\mathcal{L}_l^k} \sqrt{\frac{\sigma_w^2\gamma}{L}}\left(a_{rk}x_r^{(k^*,k)} - j a_{rk} y_r^{(k^*,k)}\right) \\ &= \sqrt{\frac{L}{N}} \sum_{k\neq k^*} z_k \sum_{l=1}^{N/L}\left(\tilde{X}_l^{(k^*,k)} - j\,\tilde{Y}_l^{(k^*,k)}\right) \end{aligned} \tag{15}$$

where $\tilde{X}_l^{(k^*,k)}$ and $\tilde{Y}_l^{(k^*,k)}$ are zero-mean truncated Gaussian distributed random variables corresponding to $X_l^{(k^*,k)}$ and $Y_l^{(k^*,k)}$ of (7) for only approved candidate subsets. It can be shown that the marginal conditional pdf of $\tilde{U}_l^{(k^*,k)} \in \left\{\tilde{X}_l^{(k^*,k)}, \tilde{Y}_l^{(k^*,k)}\right\}$ is given as (16) at the bottom of the page (see [30, p. 191]), where $\mathrm{Q}(x) = 1/\sqrt{2\pi}\int_x^\infty \exp(-u^2/2)du$ is the Q-function of the Gaussian distribution.

Using (15), the total INR at d_{k^*} can be expressed as (17), shown at the bottom of the next page. Based on the central limit theorem, both summation terms in (17) corresponding to the real and imaginary parts of the INR from each set of collaborative nodes, i.e., $\sqrt{L/N\sigma_w^2}\sum_{l=1}^{N/L}\tilde{X}_l^{(k^*,k)}$ and $\sqrt{L/N\sigma_w^2}\sum_{l=1}^{N/L}\tilde{Y}_l^{(k^*,k)}$, are zero-mean Gaussian distributed random variables with variance for both given as

$$\begin{aligned} \sigma_\Sigma^2 &= E\left\{\left(\sqrt{\frac{L}{N\sigma_w^2}}\sum_{l=1}^{N/L}\tilde{X}_l^{(k^*,k)}\right)^2\right\} \\ &= E\left\{\left(\sqrt{\frac{L}{N\sigma_w^2}}\sum_{l=1}^{N/L}\tilde{Y}_l^{(k^*,k)}\right)^2\right\} \\ &= \frac{\sigma_X^2(1-(1+\beta)e^{-\beta})}{\sigma_w^2(1-e^{-\beta})} \end{aligned} \tag{18}$$

where $\beta = \sigma_w^2\eta_{\mathrm{thr}}/2\sigma_X^2$.

Therefore, the total INR η collected at d_{k^*} from all collaborative sets is a sum of exponentially distributed random

$$f\left(\tilde{U}_l^{(k^*,k)}\middle|\,\eta\le\eta_{\mathrm{thr}}\right) = f\left(\tilde{U}_l^{(k^*,k)}\middle|\left(\tilde{X}_l^{(k^*,k)}\right)^2 + \left(\tilde{Y}_l^{(k^*,k)}\right)^2 \le \sigma_w^2\eta_{\mathrm{thr}}\right)$$
$$= \frac{1}{\sqrt{2\pi\sigma_X^2}}\left[1-\exp\left(-\frac{\sigma_w^2\eta_{\mathrm{thr}}}{2\sigma_X^2}\right)\right]^{-1}\left[1-2\,\mathrm{Q}\left(\frac{\sqrt{\sigma_w^2\eta_{\mathrm{thr}} - \left(\tilde{U}_l^{(k^*,k)}\right)^2}}{\sigma_X}\right)\right]\exp\left(-\frac{\left(\tilde{U}_l^{(k^*,k)}\right)^2}{2\sigma_X^2}\right)$$
$$|\tilde{U}_l^{(k^*,k)}| \le \sqrt{\sigma_w^2\,\eta_{\mathrm{thr}}} \tag{16}$$

variables [see (17)] and can be shown to be Erlang distributed, that is,

$$f(\eta \mid K,\alpha) = \frac{\alpha^K(\eta)^{K-1}\exp(-\alpha\eta)}{(K-1)!}, \quad \text{for } K>0,\ \eta \geq 0,\ \alpha = \frac{1}{2\sigma_\Sigma^2}. \tag{19}$$

Finally, using (19), the CCDF of the INR can be expressed in closed-form as

$$\mathbf{Pr}\{\eta \geq \eta_0\} = \sum_{k=0}^{K-1} \frac{(\alpha\eta_0)^k e^{-\alpha\eta_0}}{k!}. \tag{20}$$

C. SINR and Transmission Rate

The average SINR at the intended BS/AP d_{k^*} for the proposed multilink CB with node selection can be found as

$$\gamma_{ML}^{k^*} = \frac{E\left\{\left|\sqrt{P}\sum\limits_{r\in\mathcal{N}^{k^*}} a_{rk^*}\right|^2\right\}}{E\left\{|I(\varphi_{k^*}\,|\bigcup\mathcal{N}^{k\neq k^*})|^2\right\}+\sigma_w^2}. \tag{21}$$

Using the facts that $E\left\{\left|\sqrt{P}\sum_{r\in\mathcal{N}^{k^*}} a_{rk^*}\right|^2\right\} = P(N\sigma_a^2 + N^2m_a^2)$ and $E\left\{|I(\varphi_{k^*}|\bigcup\mathcal{N}^{k\neq k^*})|^2\right\} = 2K\sigma_I^2$ where the latter one follows from (18) with $\sigma_I^2 = \sigma_\Sigma^2\sigma_w^2$, the average SINR (21) can be rewritten as

$$\gamma_{ML}^{k^*} = \frac{P(N\sigma_a^2+N^2m_a^2)}{2K\sigma_I^2+\sigma_w^2} = \frac{\gamma\sigma_w^2(\sigma_a^2+Nm_a^2)}{2K\sigma_I^2+\sigma_w^2}. \tag{22}$$

Since $K+1$ source–destination links are used simultaneously, the transmission rate in bits/s/Hz of the multilink CB with node selection can be expressed as

$$\begin{aligned} C_{ML} &= (K+1)\log_2(1+\gamma_{ML}^{k^*}) \\ &= (K+1)\log_2\left(1+\frac{\gamma\sigma_w^2(\sigma_a^2+Nm_a^2)}{2K\sigma_I^2+\sigma_w^2}\right). \end{aligned} \tag{23}$$

Similarly, using (21), the average SINR at the intended BS/AP d_{k^*} for the multilink CB without node selection can be found as

$$\bar{\gamma}_{ML}^{k^*} = \frac{P(N\sigma_a^2+N^2m_a^2)}{2K\sigma_X^2+\sigma_w^2} = \frac{\gamma\sigma_w^2(\sigma_a^2+Nm_a^2)}{2K\sigma_X^2+\sigma_w^2} \tag{24}$$

where $E\left\{|I(\varphi_{k^*}|\bigcup\mathcal{N}^{k\neq k^*})|^2\right\} = 2K\sigma_X^2$ in this case, i.e., σ_I^2 in (22) is substituted by σ_X^2 in (24). Then the corresponding transmission rate can be expressed as

$$C'_{ML} = (K+1)\log_2\left(1+\frac{\gamma\sigma_w^2(\sigma_a^2+Nm_a^2)}{2K\sigma_X^2+\sigma_w^2}\right). \tag{25}$$

Finally, in the single-link CB case, the interference is not present and the SNR at the intended BS/AP d_{k^*} can be found as

$$\begin{aligned} \gamma_{\mathrm{SL}}^{k^*} &= \frac{E\left\{\left|\sqrt{P}\sum\limits_{r\in\mathcal{M}^{k^*}} a_{rk^*}\right|^2\right\}}{\sigma_w^2} \\ &= \frac{P(M\sigma_a^2+M^2m_a^2)}{\sigma_w^2} \\ &= \gamma((K+1)\sigma_a^2+(K+1)^2Nm_a^2) \end{aligned} \tag{26}$$

where the number of sensor nodes used in the single-link CB case is the same as the total number of sensor nodes used in all links in the multilink CB case, i.e., for fare comparison with the multilink CB case $M=(K+1)N$. Thus, the power per one collaborative sensor node is $P=\sigma_w^2\gamma/N$. Then the corresponding transmission rate is given as

$$C_{\mathrm{SL}} = \log_2(1+\gamma((K+1)\sigma_a^2+(K+1)^2Nm_a^2)). \tag{27}$$

It can be seen that although there is no interference for the single-link CB and better SNR than SINR in the multilink CB can be achieved, the single-link CB transmission rate improvement over the multilink CB is only logarithmic, while the multilink CB transmission rate improvement over the single-link CB due to multiple links is linear. Moreover, sidelobe control via node selection achieves isolation between different links in the multilink CB and, thus, the interference is minimized that leads to increased link transmission rate as well.

Finally, note that since the node selection has to be done at the deployment stage of WSN and repeated only when the network configuration changes, the transmission rate loss because of the overhead spent on node selection is insignificant since it is run in a much slower time scale than the actual data transmission. Moreover, this overhead can be controlled if necessary and depends on the size of the candidate set of nodes L and the threshold η_{thr}.

$$\begin{aligned} \eta &= \frac{1}{\sigma_w^2}\left|I\left(\varphi_{k^*}\left|\bigcup\mathcal{N}^{k\neq k^*}\right.\right)\right|^2 \\ &= \frac{L}{N\sigma_w^2}\sum_{k\neq k^*}\left(\left(\sum_{l=1}^{N/L}\tilde{X}_l^{(k^*,k)}\right)^2+\left(\sum_{l=1}^{N/L}\tilde{Y}_l^{(k^*,k)}\right)^2\right) \\ &= \sum_{k\neq k^*}\left(\left(\sqrt{\frac{L}{N\sigma_w^2}}\sum_{l=1}^{N/L}\tilde{X}_l^{(k^*,k)}\right)^2+\left(\sqrt{\frac{L}{N\sigma_w^2}}\sum_{l=1}^{N/L}\tilde{Y}_l^{(k^*,k)}\right)^2\right). \end{aligned} \tag{17}$$

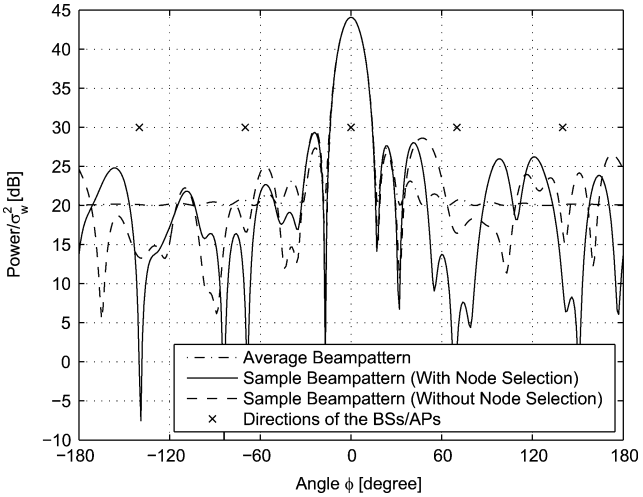

Fig. 3. Beampattern: The intended BS/AP is located at $\varphi_0 = 0^\circ$ and 4 unintended BSs/APs at directions $\varphi_1 = -140^\circ$, $\varphi_2 = -70^\circ$, $\varphi_3 = 70^\circ$, and $\varphi_4 = 140^\circ$: $M = 512$, $N = 256$, $L = 32$, and $\eta_{\text{thr}} = 10$ dB.

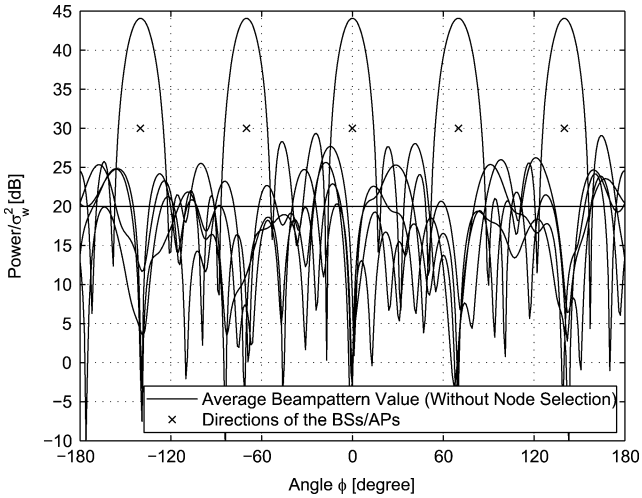

Fig. 4. Beampattern: Multilink beampatterns with BSs/APs at directions $\varphi_0 = 0^\circ$, $\varphi_1 = -140^\circ$, $\varphi_2 = -70^\circ$, $\varphi_3 = 70^\circ$, and $\varphi_4 = 140^\circ$: $M = 512$, $N = 256$, $L = 32$, and $\eta_{\text{thr}} = 10$ dB.

V. Simulation Results

In this section, we aim at demonstrating the advantages of the proposed node selection algorithm for the multilink CB beampattern sidelobe control and verifying the accuracy of the derived analytical expressions. Throughout this section the following set up is considered, unless otherwise is specified. The sensor nodes are assumed to be uniformly distributed over a disk with radius $R = 2\lambda$. The total number of sensor nodes in the coverage area of the transmitting source node is $M = 512$ and the desired number of collaborative nodes to be selected is $N = 256$. The power budget for all N collaborative nodes γ equals to 20 dB, where all power values are normalized to σ_w^2. The size of a group of candidate sensor nodes L is taken to be equal to 32 and the INR threshold value at the unintended BSs/APs is set to $\eta_{\text{thr}} = 10$ dB. The intended BS/AP is located at the direction $\varphi_0 = 0^\circ$ in all scenarios, while the direction to the unintended BS/AP is $\varphi_1 = 65^\circ$ in the scenarios with only one unintended BS/AP. In the scenarios with multiple unintended BSs/APs, the directions are defined in corresponding scenarios. Moreover, we always assume for simplicity, but without any loss of generality, that η_{thr} is the same for all BSs/APs. Indeed, the node selection is performed based on the 'accept/reject' bit from the corresponding BS/AP, that is, the threshold η_{thr} is used only at the BS/AP. Therefore, it is straightforward to use different threshold values at different BSs/APs without any change to the node selection algorithm.

A. Sample CB Beampattern

Scenario 1: In this scenario, $D = 4$ unintended BSs/APs are present and the corresponding directions are $\varphi_1 = -140^\circ$, $\varphi_2 = -70^\circ, \varphi_3 = 70^\circ$, and $\varphi_4 = 140^\circ$. Fig. 3 shows the sample beampattern corresponding to the multilink CB with node selection and compares it to the sample beampattern corresponding to the multilink CB without node selection and the average beampattern. It can be seen from the figure that the CB with node selection archives the lowest sidelobes in the directions of unintended BSs/APs, while the sidelobes of the CB without node selection are uncontrolled and high in the directions of unintended BSs/APs. Moreover, Fig. 4 shows the beampatterns of the multilink CBs with node selection for all sets of collaborative nodes. It can be seen from the figure that each beampattern has minimum interference at the directions of the mainlobes of the other beampatterns.

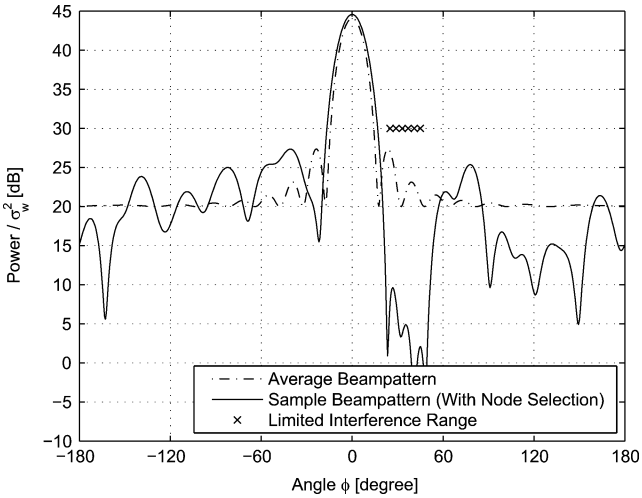

Fig. 5. Beampattern: The interference is limited in the range $\phi \in [25^\circ\ 45^\circ]$: $M = 512, N = 256, L = 32, \varphi_0 = 0^\circ$, and $\eta_{\text{thr}} = 10$ dB.

Scenario 2: In this scenario, it is required to limit the interference in the range $\phi \in [25^\circ\ 45^\circ]$. The beampattern of the CB with node selection and the average beampattern are shown in Fig. 5. It can be seen from the figure that the CB with node selection is able to achieve a beampattern with sufficiently low sidelobes over the whole range $\phi \in [25^\circ\ 45^\circ]$. Note that this case corresponds, for example, to the situation when the unintended BS/AP is actually another cluster of sensor nodes distributed over space, which, therefore, cannot be viewed as a point in space.

Scenario 3: In the last scenario, we assume that $D = 4$ unintended Bs/APs are located at the directions corresponding to

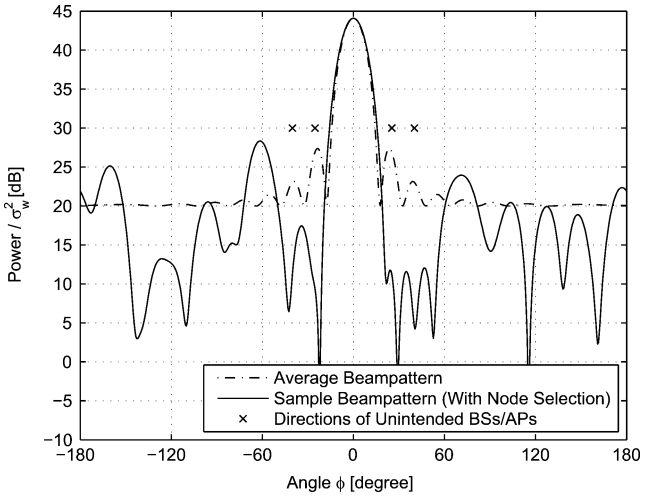

Fig. 6. Beampattern: The unintended BSs/APs are at directions corresponding to the peaks of the average beampattern: $M = 512$, $N = 256$, $L = 32$, $\varphi_0 = 0°$, and $\eta_{\rm thr} = 10$ dB.

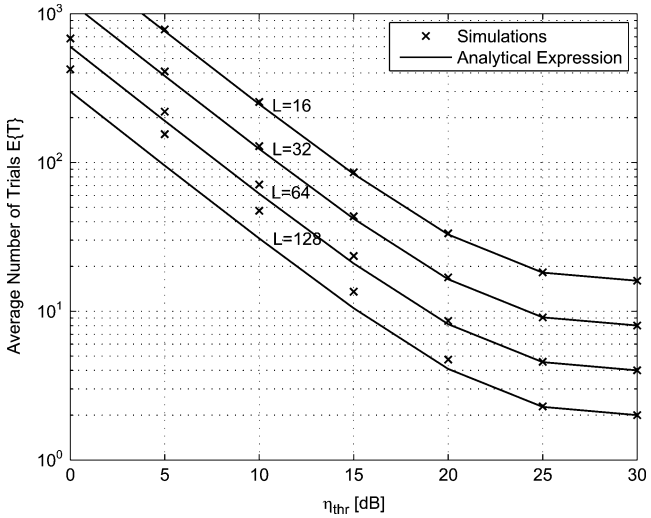

Fig. 7. Average number of trials $E\{T\}$ versus threshold $\eta_{\rm thr}$: $M = 512$, $N = 256$, $\varphi_0 = 0°$, and $\varphi_1 = 65°$.

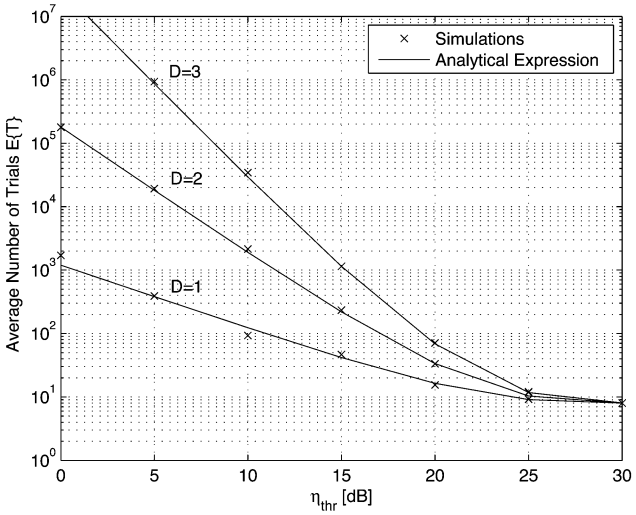

Fig. 8. Average number of trials $E\{T\}$ versus threshold $\eta_{\rm thr}$ for different values of D: $M = 512$, $N = 256$, $L = 32$, and $\varphi_0 = 0°$.

the largest peaks of the average beampattern. Therefore, the locations of the unintended BSs/APs are actually the worst possible locations in terms of the corresponding average interference levels. Fig. 6 shows the average beampattern and the beampattern of the CB with node selection. As it can be seen from the figure, using the node selection, we can achieve minimum interference levels at the directions of unintended BSs/APs even in this case.

B. Average Number of Trials

The two parameters in the node selection algorithm are the INR threshold $\eta_{\rm thr}$ and the size L of the candidate set of nodes $\mathcal{L}^{k^*}$ for fixed N.

In this example, the INR threshold value changes in the range $\eta_{\rm thr} = [0\ 30]$ dB. The parameters of the Gaussian distribution corresponding to the lognormal distribution of the channel coefficients are $m = 0$ and $\sigma^2 = 0.2$. Monte Carlo simulations are carried over using 1000 runs to obtain average results.

Fig. 7 demonstrates the effect of the threshold $\eta_{\rm thr}$ on the average number of trials required to select the set of collaborative nodes $\mathcal{N}^k$ using the sets of candidate nodes of different sizes $L \in \{16,\ 32,\ 64,\ 128\}$. It can be seen from the figure that the curves obtained using the closed-form expression (13) for the average number of trials are in good agreement with the simulation results. It can also be seen that by decreasing the threshold $\eta_{\rm thr}$, the number of trials increases. Moreover, the number of trials for fixed N can be controlled using L. Indeed, as L increases, the number of trials decreases.

In our next example, we study the effect of the number of unintended BSs/APs D to the performance of the node selection algorithm. In Fig. 8, the average number of trials is plotted versus the threshold $\eta_{\rm thr}$ for different values of $D \in \{1,\ 2,\ 3\}$. It can be seen from this figure that as D increases, the average number of trials of the node selection algorithm increases exponentially if the threshold $\eta_{\rm thr}$ is low. Finally, it can be observed that the analytical and simulation results are in a good agreement with each other.

C. CCDF of the Beampattern Level

Fig. 9 depicts the probability that the interference exceeds certain level, i.e., it shows the CCDF of interference for different values of $\eta_{\rm thr} \in \{-5,\ 0,\ 5,\ 10\}$. In addition, Fig. 10 illustrates the CCDF of the interference for different numbers of active collaborative sets $K + 1 = 2,\ 3$, or 4. It can be seen from Fig. 9 that the CCDF of the interference increases as $\eta_{\rm thr}$ increases. Moreover, as can be observed from Fig. 10, the CCDF of the interference increases if K increases. The latter fact agrees with the intuition that for larger number of collaborative sets transmitting simultaneously, the overall received interference by all BSs/APs must be higher. The simulation results in both figures closely agree with our analytical results as well.

D. SINR and Transmission Rate

In Fig. 11, the SNR of the single-link CB (22) and the SINR for one link of the multilink CB with node selection (24) and without node selection (26) are plotted versus the

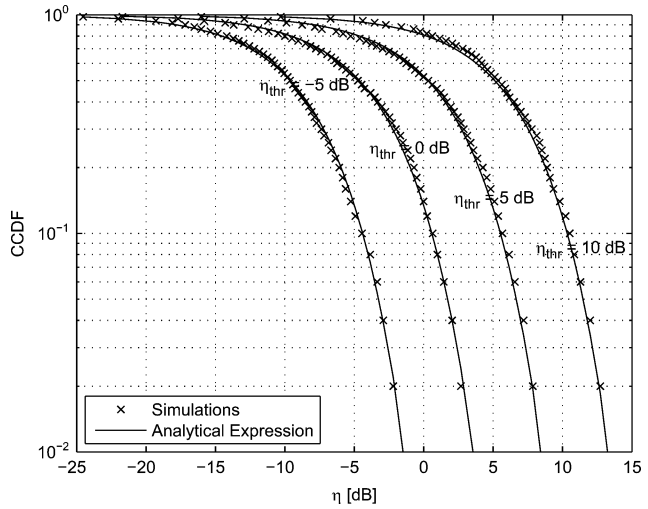

Fig. 9. The CCDF of the INR for different values of the threshold $\eta_{\rm thr}$: $M = 512$, $N = 256$, $L = 32$, $\varphi_0 = 0°$, and $\varphi_1 = 65°$.

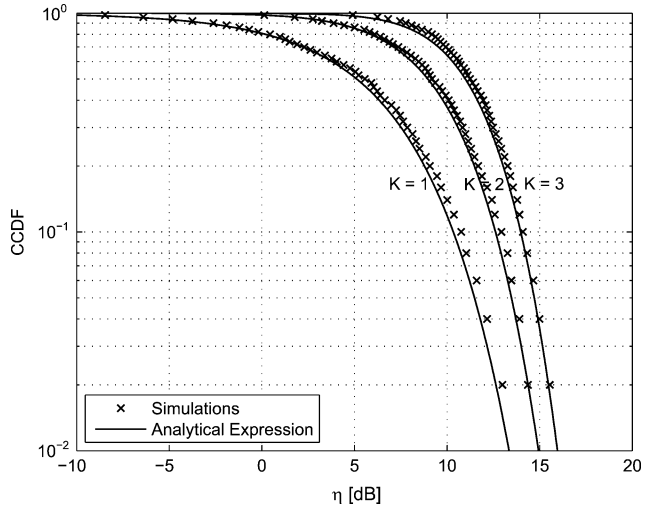

Fig. 10. The CCDF of the INR for different values of K: $M = 512, N = 256$, $L = 32, \varphi_0 = 0°$, and $\eta_{\rm thr} = 10$ dB.

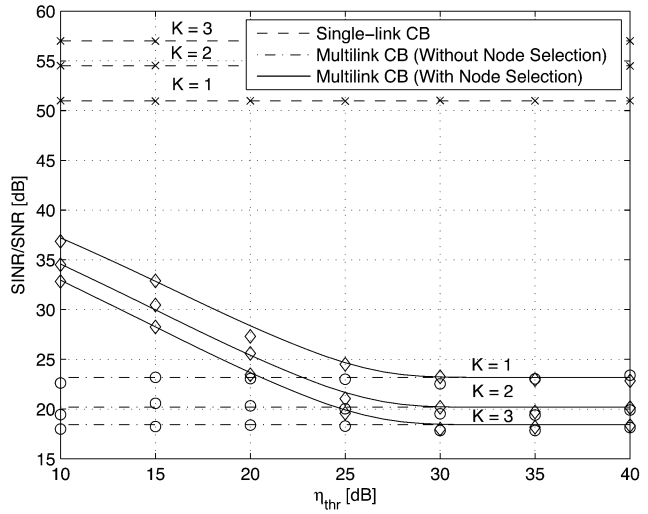

Fig. 11. The SNR of the single-link CB and the SINR of the multilink CBs with and without node selection for different values of K: $M = 512$, $N = 256$, $L = 32$, and $\varphi_0 = 0°$.

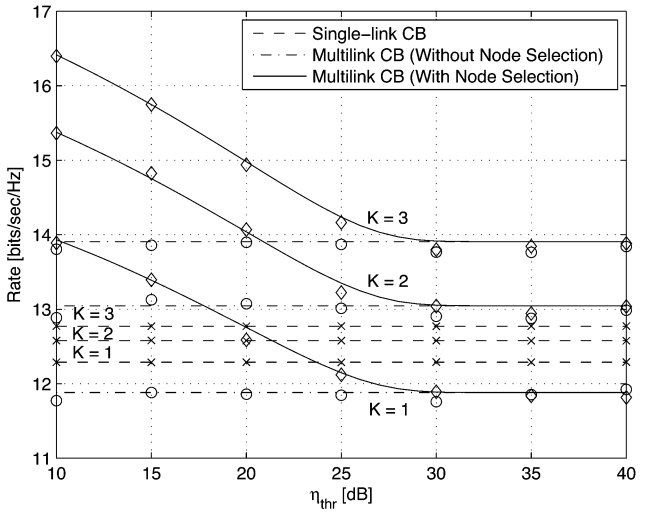

Fig. 12. The transmission rate of the single- and multilink CBs with and without node selection for different values of K: $M = 512$, $N = 256$, $L = 32$, and $\varphi_0 = 0°$.

threshold value $\eta_{\rm thr}$ for different numbers of collaborative sets $K + 1 = 2,\ 3$, or 4 and compared with the simulation results. Since the single-link CB does not have interference, it can be seen that it achieves higher SNR than the SINR achieved by one link of the multilink CB. Moreover, it can be seen from this figure that the SINR of the multilink CB with node selection increases as the threshold $\eta_{\rm thr}$ decreases. The SINR is lower for the multilink CB if larger number of collaborative sets, $K + 1$, is transmitting simultaneously because of the increased interference. In the case of the single-link CB, larger K results in increase of M since $M = (K + 1)N$. Therefore, more collaborative nodes are available for the single-link CB with larger K and the SNR increase can be observed.

In Fig. 12, the corresponding total transmission rates computed according to the expressions (23), (25), and (27) are plotted and compared with the simulation results. It can be seen from this figure that for $K > 1$, the transmission rate of the multilink CB with and without node selection is larger than that achieved by the single-link CB. Moreover, higher transmission rate can be achieved by the multilink CB with node selection as the threshold $\eta_{\rm thr}$ decreases.

Comparing Figs. 7 and 12 to each other, we can observe a tradeoff between the average number of trials required for node selection and the achieved transmission rate. Particularly, higher transmission rate is achieved by using smaller values of $\eta_{\rm thr}$ in the multilink CB with node selection or larger number of collaborative sets transmitting simultaneously (see Fig. 12). This transmission rate increase is archived at the expense of larger number of trials in the selection algorithm (see Figs. 7 and 8).

VI. Conclusion

Node selection has been introduced for the multilink CB sidelobe control in the context of WSNs and an efficient algorithm with low overhead has been developed and analyzed. The expressions for the average number of trials required for the proposed node selection algorithm and the CCDF of the interference of the multilink CB with node selection have been derived.

Moreover, the transmission rate for the multilink CB with and without node selection has been analyzed and compared to that of the single-link CB. From both the analytical and simulation results, we have seen that the multilink CB with node selection has perfect interference suppression capabilities as compared to the multilink CB without node selection. It has been also shown that the transmission rate achievable by the multilink CB with node selection is significantly higher than that of the multilink CB without node selection and single-link CB. Although our theoretical analysis is approximate, the numerical results show close agreement with our analytical results.

APPENDIX
DERIVATION OF THE MEAN AND VARIANCE OF $x_r^{(k^*,k)}$ AND $y_r^{(k^*,k)}$

Let the angles θ_r^k and $\theta_r^{k^*}$ be uniform distributed in the interval $[-\pi,\ \pi]$, i.e., $\theta \sim \mathcal{U}[-\pi,\ \pi]$. Since the mod-$2\pi$ sum of two uniform r.v.'s on $[0,\ 2\pi]$ is again uniform on $[0,\ 2\pi]$, it can be found that the difference $\Delta = \theta_r^k - \theta_r^{k^*}$ has uniform distribution on $[0,\ 2\pi]$. Using the equality $u = \mathcal{R}\left\{e^{j\Delta}\right\} = \cos(\Delta)$, the distribution of $u \in \left\{x_r^{(k^*,k)}, y_r^{(k^*,k)}\right\}$ can be found as

$$f(u) = \frac{1}{\pi\sqrt{1-u^2}}. \tag{28}$$

The mean can be then easily found as $m_u = 0$ and the variance as $\sigma_u^2 = 0.5$. Similar result can be also derived for $u \triangleq \mathcal{I}\left\{e^{j\Delta}\right\} = \sin(\Delta)$ in the same way.

ACKNOWLEDGMENT

The authors wish to thank the anonymous reviewers for their helpful comments and suggestions, which led to presentation improvements and addition of the transmission rate analysis for the multilink CB with and without node selection.

REFERENCES

[1] D. Culler, D. Estrin, and M. Srivastava, "Overview of sensor networks," *Computer*, vol. 37, no. 8, pp. 41–49, Aug. 2004.
[2] J. Yindi and H. Jafarkhani, "Network beamforming using relays with perfect channel information," in *Proc. IEEE ICASSP*, Apr. 2007, pp. 473–476.
[3] H. Ochiai, P. Mitran, H. V. Poor, and V. Tarokh, "Collaborative beamforming for distributed wireless ad-hoc sensor networks," *IEEE Trans. Signal Process.*, vol. 53, pp. 4110–4124, Nov. 2005.
[4] M. F. A. Ahmed and S. A. Vorobyov, "Collaborative beamforming for wireless sensor networks with Gaussian distributed sensor nodes," *IEEE Trans. Wireless Commun.*, vol. 8, no. 2, pp. 638–643, Feb. 2009.
[5] R. Mudumbai, B. Wild, U. Madhow, and K. Ramchandran, "Distributed beamforming using 1 bit feedback: From concept to realization," in *Proc. Ann. Allerton Conf. Commun. Contr. Comput.*, Sep. 2006, pp. 1020–1027.
[6] Q. Wang and K. Ren, "Time-slotted round-trip carrier synchronization in large-scale wireless networks," in *Proc. IEEE ICC*, Beijing, May 2008, pp. 5087–5091.
[7] D. R. Brown and H. V. Poor, "Time-slotted round-trip carrier synchronization for distributed beamforming," *IEEE Trans. Signal Process.*, vol. 56, pp. 5630–5643, Nov. 2008.
[8] L. Dong, A. P. Petropulu, and H. V. Poor, "A cross-layer approach to collaborative beamforming for wireless *ad-hoc* networks," *IEEE Trans. Signal Process.*, vol. 56, pp. 2981–2993, Jul. 2008.
[9] Y. Lo, "A mathematical theory of antenna arrays with randomly spaced elements," *IEEE Trans. Antennas Propag.*, vol. 12, no. 3, pp. 257–268, May 1964.
[10] A. S. Shifrin, *Statistical Antenna Theory*. New York: Golem , 1971.
[11] M. F. A. Ahmed and S. A. Vorobyov, "Performance characteristics of collaborative beamforming for wireless sensor networks with Gaussian distributed sensor nodes," in *Proc. IEEE ICASSP*, Las Vegas, NV, Mar.-Apr. 2008, pp. 3249–3252.
[12] M. F. A. Ahmed and S. A. Vorobyov, "Beampattern random behavior in wireless sensor networks with Gaussian distributed sensor nodes," in *Proc. Canad. Conf. Electr. Comp. Eng.*, May 2008, pp. 257–260.
[13] K. Zarifi, S. Affes, and A. Ghrayeb, "Collaborative null-steering beamforming for uniformly distributed wireless sensor networks," *IEEE Trans. Signal Process.*, vol. 58, no. 3, pp. 1889–1903, Mar. 2010.
[14] H. L. Van Trees, *Optimum Array Processing*. New York: Wiley, 2002.
[15] J. Liu, A. B. Gershman, Z. Q. Luo, and K. M. Wong, "Adaptive beamforming with sidelobe control: A second-order cone programming approach," *IEEE Signal Process. Lett.*, vol. 10, pp. 331–334, Nov. 2003.
[16] K. L. Bell and H. L. Van Trees, "Adaptive and non-adaptive beampattern control using quadratic beampattern constraints," in *Proc. 33rd Asilomar Conf. Signals, Syst., Comput.*, Pacific Grove, CA, 1999, pp. 486–490.
[17] D. T. Hughes and J. G. McWhirter, "Sidelobe control in adaptive beamforming using a penalty function," in *Proc. ISSPA*, Gold Coast, Australia, 1996.
[18] V. Havary-Nassab, S. Shahbazpanahi, A. Grami, and L. Zhi-Quan, "Distributed beamforming for relay networks based on second-order statistics of the channel state information," *IEEE Trans. Signal Process.*, vol. 56, pp. 4306–4316, Sep. 2008.
[19] M. F. A. Ahmed and S. A. Vorobyov, "Node selection for sidelobe control in collaborative beamforming for wireless sensor networks," in *Proc. IEEE 10th SPAWC Workshop*, Perugia, Jun. 2009, pp. 519–523.
[20] I. Cosovic and T. Mazzoni, "Suppression of sidelobes in OFDM systems by multiple-choice sequences," *Eur. Trans. Telecommun.*, vol. 17, no. 6, pp. 623–630, Jun. 2006.
[21] P. Vandewalle, J. Kovacevic, and M. Vetterli, "Reproducible research in signal processing—What, why, and how," *IEEE Signal Process. Mag.*, vol. 26, no. 3, pp. 37–47, May 2009.
[22] J. M. Molina-Garcia-Pardo, A. Martinez-Sala, M. V. Bueno-Delgado, E. Egea-Lopez, L. Juan-Llacer, and J. Garca-Haro, "Channel model at 868 MHz for wireless sensor networks in outdoor scenarios," *IEEE J. Commun. Netw.*, vol. 7, no. 4, pp. 401–407, Dec. 2005.
[23] G. Zhou, T. He, S. Krishnamurthy, and J. A. Stankovic, "Models and solutions for radio irregularity in wireless sensor networks," *ACM Trans. Sens. Netw.*, vol. 2, no. 2, pp. 221–262, May 2006.
[24] E. L. Crow and K. Shimizu, *Lognormal Distributions: Theory and Applications*. Boca Raton, FL: CRC , 1987.
[25] C. Lin, V. V. Veeravalli, and P. M. Sean, Distributed beamforming with feedback: Convergence analysis Jul. 2008 [Online]. Available: http://arxiv.org/abs/0806.3023
[26] A. P. Petropulu, L. Dong, and H. V. Poor, "Weighted cross-layer cooperative beamforming for wireless networks," *IEEE Trans. Signal Process.*, vol. 57, pp. 3240–3252, Aug. 2009.
[27] R. Lin and A. P. Petropulu, "A new wireless network medium access protocol based on cooperation," *IEEE Trans. Signal Process.*, vol. 53, pp. 4675–4684, Dec. 2005.
[28] Y. Hailong, A. P. Petropulu, Y. Xinhua, and T. Camp, "A novel location relay selection scheme for ALLIANCES," *IEEE Trans. Veh. Technol.*, vol. 57, no. 2, pp. 1272–1284, Mar. 2008.
[29] D. C. Montgomery and G. C. Runger, *Applied Statistics and Probability for Engineers*. Hoboken, NJ: Wiley, 2007.
[30] C. W. Helstrom, *Probability and Stochastic Processes for Engineers*. New York: Macmillan, 1984.

Mohammed F. A. Ahmed (S'08) received the B.Sc. degree with honors in electronics and communications engineering and the M.Sc. degree in communications engineering from Assiut University, Assiut, Egypt, in 2001 and 2004, respectively.

From 2001 to 2006, he was with the Department of Electrical Engineering, Assiut University, as an Assistant Lecturer. Since September 2006, he has been working toward the Ph.D. degree in electrical engineering with the University of Alberta, Edmonton, AB, Canada. His research interests are in collaborative beamforming, cooperative communications, and statistical and array signal processing.

Sergiy A. Vorobyov (M'02–SM'05) received the M.S. and Ph.D. degrees in systems and control from Kharkiv National University of Radio Electronics, Ukraine, in 1994 and 1997, respectively.

Since 2006, he has been with the Department of Electrical and Computer Engineering, University of Alberta, Edmonton, AB, Canada, where he has become an Associate Professor in 2010. Since his graduation, he also occupied various research and faculty positions in Kharkiv National University of Radio Electronics, Ukraine, Institute of Physical and Chemical Research (RIKEN), Japan, McMaster University, Canada, Duisburg-Essen and Darmstadt Universities, Germany, and Joint Research Institute, Heriot-Watt and Edinburgh Universities, U.K. His research interests include statistical and array signal processing, applications of linear algebra, optimization, and game theory methods in signal processing and communications, estimation, detection, and sampling theories, and cognitive systems.

Dr. Vorobyov is a recipient of the 2004 IEEE Signal Processing Society Best Paper Award, 2007 Alberta Ingenuity New Faculty Award, and other research awards. He was an Associate Editor for the IEEE TRANSACTIONS ON SIGNAL PROCESSING (2006–2010) and for the IEEE SIGNAL PROCESSING LETTERS (2007–2009). He is a member of Sensor Array and Multi-Channel Signal Processing Technical Committee of the IEEE Signal Processing Society.